

Centralized Identification of Imbalances in Power Networks with Synchrophasor Data

Tirza Routtenberg *Member, IEEE* and Yonina C. Eldar, *Fellow, IEEE*

Abstract—The problem of bus imbalance identification in a three-phase power network using a phasor measurement unit (PMU) is considered. We propose new algorithms to identify and localize imbalances occurring at any location in the power grid, based only on single-phase PMU data. First, we develop a technique using the minimum description length (MDL) criterion that is carried out at the control center. The centralized MDL methodology is time consuming and has computational complexity that grows exponentially with the network size. Therefore, we next develop a Projected Orthogonal Matching Pursuit (POMP) algorithm, which is a low-complexity method for bus imbalance identification in large-scale power networks implemented at the control center. POMP is a computationally efficient compressive sensing technique that exploits the sparse structure of the voltage measurements. The proposed methods are validated through three case studies: a two-port π -model, an IEEE-14 bus system, and an IEEE 118-bus system. Simulations show that our networked algorithms, MDL and POMP, obtain improved performance over local bus-level identification techniques. The performance of POMP is close to that of centralized MDL, with the advantage of being applicable to large-scale networks.

Index Terms—Signal detection, phasor measurement unit (PMU), unbalanced power system, smart grid, multi-area state estimator, networked identification of imbalances, minimum description length (MDL), Orthogonal Matching Pursuit (OMP).

I. INTRODUCTION

Three-phase power systems frequently suffer from imbalances, such as load imbalances [1]. These may be precursors to more serious contingencies leading to blackouts, excessive losses, insulation degradation, and production interruptions [2], [3]. In addition, system imbalance degrades fault location accuracy [4] and state estimation performance, both in terms of bias [5] and error covariance matrices [6]. Thus, imbalance must be detected and compensated for. The use of modern devices, such as phasor measurement units (PMUs), is highly desirable for modern power systems as it facilitates rapid detection of contingencies and faults and provides accurate state and frequency estimation [1].

Traditionally, most energy management system (EMS) functions, such as state estimation, are carried out at the central unit, based on the full network data. While three-phase measurements of power and voltages are available at the local measurement device level, and, in principle, can be transmitted, only the positive sequence components are typically reported to the control center, due to communication and processing limitations. Existing methods for voltage imbalance detection

are based on two- or three-phase sequences and are performed locally at the bus level. The derivation of enhanced imbalance identification methods that use single-phase networked data is crucial for obtaining an accurate system model and high power quality. Such processing methods should be able to absorb the increasing number of available measurements, while retaining low communication capacity and low computational complexity.

The symmetrical components transformation converts three phase-measurements into a positive, a negative and a zero sequence. In balanced scenarios, it produces a significant value only in the positive sequence, since all phases are rotated to be added in-phase [2], [7]. Thus, monitoring the power system and developing state estimation methods are usually based on the positive sequence and assume that the network is balanced and can be represented by a single-phase equivalent (e.g. [1] and [8]–[10]). Recently, new state and frequency estimation approaches have also been proposed for different unbalanced system models and scenarios [11]–[16].

Classical detection of imbalances is based on measures such as the voltage unbalance factor (VUF) [17], [18], the phase voltage unbalance factor [19], and the complex VUF [20], [21]. A smart meter for voltage imbalance detection is described in [22]. In [23] a hazard-based model was introduced to predict the three-phase imbalance based on historical status data. New bus-level parametric imbalance detection methods that outperform VUF in terms of probability of error have recently been proposed, based on the generalized likelihood ratio test (GLRT) [13], [24] and the generalized locally most powerful test (GLMP) [25], [26]. For networked identification of imbalances, a non-parametric VUF approach is derived in [3], based on distribution system state estimation (DSSE) in a network. A GLRT-based test and cumulative sum (CUSUM) approach have been developed in [27] for change-detection of the imbalance condition. The VUF, GLRT, GLMP, and networked-DSSE methods are all based on two- or three-phase data that are usually not available at the control center in current networks. In contrast, our proposed parametric techniques employ networked single-phase data, and thus the need for additional communication and processing costs is avoided.

In this paper, we formulate the identification of unbalanced buses as a model order selection problem. It is well known that compressive sensing (CS) can be used to treat model order selection and parameter estimation problems with significant reduction in computational complexity [28]. Reconstruction of sparse signals and CS techniques have become very popular in the last two decades (see e.g. [29]–[31] and references therein). In power systems, CS algorithms [32] have been proposed in the context of multi-line outage identification in transmission networks [33]–[35], gross error identification [36], bad data

T. Routtenberg is with Department of Electrical and Computer Engineering, Ben-Gurion University of the Negev, Beer-Sheva 84105, Israel. Email: tirzar@bgu.ac.il. Y. C. Eldar is with the Department of Electrical Engineering, Technion-Israel Institute of Technology, Haifa 32000, Israel. Email: yonina@ee.technion.ac.il. The research of T. Routtenberg was partially supported by the ISRAEL SCIENCE FOUNDATION (ISF), Grant No. 1173/16.

detection [37], and detection of false data injection attacks [38]. Here we show that sparsity and CS techniques can also be exploited for imbalance identification.

In this paper, we consider the problem of voltage imbalance identification in a three-phase power network by using the PMU outputs. The main contributions of this work are as follows. First, we develop a statistical *networked* measurement model, which is the first published model that shows that unbalanced buses can be identified by using only the positive sequence. Second, we derive a networked algorithm for identification of unbalanced buses based on the MDL method [39], [40]. A byproduct of the proposed networked MDL technique, which is performed at the control center, is the centralized maximum likelihood (ML) state estimators. Third, since the centralized MDL approach is time consuming, we develop two low-complexity identification methods for large-scale power networks: 1) a decentralized detection methodology, where MDL and state estimation are performed separately at each bus; and 2) a networked Projected Orthogonal Matching Pursuit (POMP) method, which is a computationally efficient CS technique [31], [32] that exploits the sparsity of the negative sequence in the proposed model and is efficacious for solving large-scale problems [41]. Finally, we conduct numerical simulations demonstrating that the proposed centralized MDL and POMP algorithms outperform local approaches. An early version of the proposed minimum description length (MDL) approach was presented in [42] and was extended in [43] to a classifier that is able to identify the number of nonzero symmetrical components and to classify the signal into four different imbalance scenarios.

The remainder of the paper is organized as follows. Section II presents the model for the networked PMU output in an unbalanced system. The MDL approach for identification of unbalanced buses is derived in Section III. In Section IV two low-complexity identification methods are developed: 1) decentralized identification, in which the imbalance detection is performed separately at each bus; and 2) centralized identification based on low-complexity CS techniques. The proposed methods are evaluated via simulations in Section V. Conclusions appear in Section VI.

In the rest of this paper, vectors are denoted by boldface lowercase letters and matrices by boldface uppercase letters. The superscripts $(\cdot)^*$, $(\cdot)^T$, $(\cdot)^H$, and $(\cdot)^{-1}$ denote the conjugate, transpose, conjugate transpose, and matrix inverse operators, respectively. For a full-rank matrix \mathbf{A} , \mathbf{A}^\dagger denotes the Moore-Penrose pseudo-inverse given by $\mathbf{A}^\dagger \triangleq (\mathbf{A}^H \mathbf{A})^{-1} \mathbf{A}^H$. The operators $\text{Real}\{\cdot\}$ and $\text{Imag}\{\cdot\}$ denote the real and imaginary parts of their arguments, respectively. Given a vector $\mathbf{u} = [u_1, \dots, u_n]^T$ and a set $\mathcal{S} = \{i_1, \dots, i_L\} \subset \{1, \dots, n\}$ of integers, $\mathbf{u}_{\mathcal{S}} = [u_{i_1}, \dots, u_{i_L}]^T$ denotes the subvector of \mathbf{u} indexed by \mathcal{S} . Similarly, given a matrix \mathbf{Q} and a set \mathcal{S} , $\mathbf{Q}_{\mathcal{S}}$ is the submatrix whose columns are indexed by \mathcal{S} . The Euclidean ℓ_2 -norm is denoted by $\|\cdot\|_2$. Finally, variables are cataloged in the nomenclature Table.

II. SYSTEM MODEL AND PROBLEM FORMULATION

We consider a power network that is observable through PMUs installed at all buses or at optimal locations [44]. The proposed method aims to identify the unbalanced buses among the measured buses, based only on the positive sequence at the

NOMENCLATURE

N	Samples per cycle in the time domain
M	Buses in the power network
K	Buses with PMU in the power network
L	Transmission lines measured by the PMU
ω_0	Nominal grid frequency
Δ	Frequency deviation
$\hat{\Delta}$	Frequency deviation estimator
α	$e^{j2\pi/3}$
γ	$\frac{2\pi}{N}$
$V_{a,m}, V_{b,m}, V_{c,m}$	Three-phase voltage magnitudes of the m th bus
$\varphi_{a,m}, \varphi_{b,m}, \varphi_{c,m}$	Three-phase voltage phases of the m th bus
$v_{a,m}[n], v_{b,m}[n], v_{c,m}[n]$	Three-phase sampled voltages at time n
$v_{+,m}[n]$	Voltage at the m th bus at time n
$\mathbf{z}[n]$	Augmented measurement vector at the control center at time n
$\mathbf{v}_+[n]$	Voltage positive-sequence measurement vector at time n
$\mathbf{w}[n]$	Networked complex circularly symmetric Gaussian noise at time n
σ^2	Noise variance
\mathbf{B}	System matrix
\mathbf{Y}	Current to voltage phasor transformation matrix
\mathbf{I}_K	$K \times K$ identity matrix
$C_{+,m}, C_{-,m}$	Positive and negative phasors at the m th bus
\mathbf{c}_+	$[C_{+,1}, \dots, C_{+,M}]^T$
\mathbf{c}_-	$[C_{-,1}^*, \dots, C_{-,M}^*]^T$
$\hat{\mathbf{c}}_+^{(i)}, \hat{\mathbf{c}}_-^{(i)}$	ML state estimators under the i th hypothesis
$\hat{\mathbf{c}}_+^{(\text{POMP})}, \hat{\mathbf{c}}_-^{(\text{POMP})}$	State estimators obtained by POMP
$T_i^{(\text{MDL})}$	MDL statistic for central identification
$T_m^{(\text{local})}$	Statistic for local detection at the m th bus

control center. For instance, in the IEEE 14-bus test system, which is shown in Fig. 1 as a single line diagram, the PMUs are located at buses 2, 6, 7, 9, which results in an observable system [44]. Similar to [2], loading imbalances are found at the buses with load 4, 5 and 9. The goal is to use the PMU voltage and current measurements to locate the unbalanced buses.

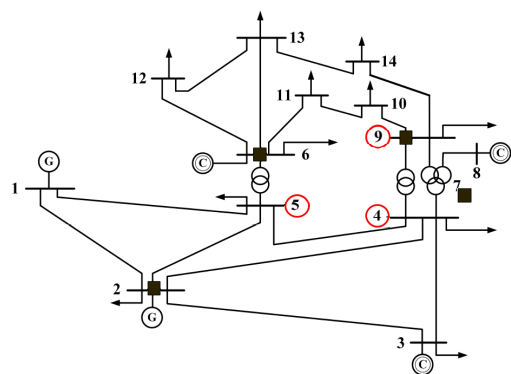


Fig. 1. IEEE-14 bus system: Rectangles represent PMU locations; Red circles represent unbalanced buses.

In this section, we present the mathematical model of the PMU positive sequence output. In Subsection II-A, we describe the conventional model (e.g. [1] and [45]) for single-bus measurements. In Section II-B, we derive a model for the total measurements at the control center, obtained from the M PMU-equipped buses, based on the single-bus measurement models.

A. Single-bus PMU measurement model

The voltages in a three-phase power system at each bus are assumed to be pure sinusoidal signals of frequency $\omega_0 + \Delta$, where ω_0 is the known nominal frequency (100π or 120π) and Δ is the frequency deviation. Due to system inertia, the frequency can be assumed identical over the network of measurement nodes. The magnitudes and phases of the three voltages of the m th bus are denoted by $V_{a,m}, V_{b,m}, V_{c,m} \geq 0$ and $\varphi_{a,m}, \varphi_{b,m}, \varphi_{c,m} \in [0, 2\pi]$, respectively, for any $m = 1, \dots, M$. Therefore, the sampled three-phase voltages can be represented in discrete time form as

$$v_{a,m}[n] = V_{a,m} \cos\left(\gamma \frac{\omega_0 + \Delta}{\omega_0} n + \varphi_{a,m}\right) \quad (1)$$

$$v_{b,m}[n] = V_{b,m} \cos\left(\gamma \frac{\omega_0 + \Delta}{\omega_0} n + \varphi_{b,m}\right) \quad (2)$$

$$v_{c,m}[n] = V_{c,m} \cos\left(\gamma \frac{\omega_0 + \Delta}{\omega_0} n + \varphi_{c,m}\right), \quad (3)$$

for any $n = 0, \dots, N - 1$, where $\gamma \triangleq \frac{2\pi}{N}$ and the sampling rate is N times per cycle of the nominal frequency, ω_0 . For the sake of simplicity, the sequences are presented here without noise. The noise statistic is discussed in the networked model.

In current systems, while all three-phase voltages and currents are monitored by PMUs, usually only the positive sequence is transmitted to the control center [2], [8]. The positive sequence voltage, aka the ‘‘space vector’’ [46], is calculated from three-phase voltages by using the symmetrical component transformation ([1] pp. 63-67, [47]):

$$v_{+,m}[n] = \frac{1}{3} (v_{a,m}[n] + \alpha v_{b,m}[n] + \alpha^2 v_{c,m}[n]), \quad (4)$$

for any $n = 0, 1, \dots, N - 1$, where $\alpha = e^{j2\pi/3}$. By substituting (1)-(3) in (4) and using the trigonometric identity $\cos a = \frac{1}{2}e^{ja} + \frac{1}{2}e^{-ja}$, we obtain the voltage signal at the m th bus:

$$v_{+,m}[n] = e^{j\gamma \frac{\omega_0 + \Delta}{\omega_0} n} C_{+,m} + e^{-j\gamma \frac{\omega_0 + \Delta}{\omega_0} n} C_{-,m}^*, \quad (5)$$

for any $n = 0, \dots, N - 1$ and any bus $m = 1, \dots, M$, where

$$C_{+,m} \triangleq \frac{1}{6} (V_{a,m} e^{j\varphi_{a,m}} + \alpha V_{b,m} e^{j\varphi_{b,m}} + \alpha^2 V_{c,m} e^{j\varphi_{c,m}}) \quad (6)$$

$$C_{-,m} \triangleq \frac{1}{6} (V_{a,m} e^{j\varphi_{a,m}} + \alpha^2 V_{b,m} e^{j\varphi_{b,m}} + \alpha V_{c,m} e^{j\varphi_{c,m}}) \quad (7)$$

are the positive and negative sequence phasors at the m th bus.

The m th bus is perfectly balanced or symmetrical if $V_{a,m} = V_{b,m} = V_{c,m}$ and $\varphi_{a,m} = \varphi_{b,m} + \frac{2\pi}{3} = \varphi_{c,m} - \frac{2\pi}{3}$. By substituting these values in (7), it can be verified that for a perfectly balanced bus $C_{-,m} = 0$. Therefore, the model for a balanced system is given by

$$v_{+,m}[n] = e^{j\gamma \frac{\omega_0 + \Delta}{\omega_0} n} C_{+,m}, \quad n = 0, \dots, N - 1. \quad (8)$$

For a balanced system, the positive sequence, $v_{+,m}[n]$, contains the same information as (1)-(3). Consequently, only the positive sequence components are typically reported to the control center. However, in the presence of imbalances and faults, the negative and zero sequences [1] are nonzero [8] and the three-phase measurements from (1)-(3) cannot be reconstructed from the positive sequence.

Existing methods for imbalance detection are based on two- or three-phase sequences. That is, in addition to the positive sequence in (4), the negative sequence

$$v_{-,m}[n] = \frac{1}{3} (v_{a,m}[n] + \alpha^2 v_{b,m}[n] + \alpha v_{c,m}[n]), \quad (9)$$

$n = 0, \dots, N - 1$, is required for implementing existing local and networked methods (e.g. [3], [13], [17], [18], [24]–[26]). The different models in (5) and (8) indicate that voltage imbalance is detectable in the time domain, even locally, by using only the positive sequence model with at least $N = 2$ measurements. In this work we develop local and networked methods that are based on single-phase data. To the best of our knowledge, this is the first published model that shows that unbalanced buses can be identified by using only the single-phase positive sequence.

B. Networked measurement model

The measurement set at the control center consists of the positive-sequence measurements obtained by the K PMUs. In addition to measuring the K bus voltages where the PMUs are installed, PMUs measure the L current phasors in lines connected to these buses. Thus, the noisy measurement vector that is received at the control center is given by [8]

$$\mathbf{z}[n] = \mathbf{B}\mathbf{v}_+[n] + \mathbf{w}[n], \quad n = 0, \dots, N - 1, \quad (10)$$

where $\mathbf{z}[n] \in \mathbb{C}^{(K+L)}$ contains K voltage and L current measurements, and the system matrix is given by $\mathbf{B} \triangleq \begin{bmatrix} \mathbf{A} \\ \mathbf{Y} \end{bmatrix} \in \mathbb{C}^{(K+L) \times M}$, in which \mathbf{A} is a $K \times M$ matrix with columns from an identity matrix representing the places with a PMU and $\mathbf{Y} \in \mathbb{C}^{L \times M}$ is a function of admittance and topology factors (e.g. Chapter 7 in [1]). The voltage vector, $\mathbf{v}_+[n] \triangleq [v_{+,1}[n], \dots, v_{+,M}[n]]^T$, is the system state vector at time n , in which $v_{+,m}[n]$ is the voltage at the m th bus at time n for any $m = 1, \dots, M$. The noise vector sequence $\mathbf{w}[n]$, $n = 0, \dots, N - 1$, is assumed to be a time-independent zero-mean complex circularly symmetric Gaussian noise sequence with known covariance matrix, $\sigma^2 \mathbf{I}_{K+L}$. In the following, we assume that the system is perfectly observable by these PMUs, i.e. \mathbf{B} is a full column rank matrix and $K + L \geq M$.

By substituting $v_{+,m}[n]$ from (5) in (10), one obtains

$$\mathbf{z}[n] = e^{j\gamma \frac{\omega_0 + \Delta}{\omega_0} n} \mathbf{B}\mathbf{c}_+ + e^{-j\gamma \frac{\omega_0 + \Delta}{\omega_0} n} \mathbf{B}\mathbf{c}_- + \mathbf{w}[n], \quad (11)$$

where $\mathbf{c}_+ \triangleq [C_{+,1}, \dots, C_{+,M}]^T$ and $\mathbf{c}_- \triangleq [C_{-,1}^*, \dots, C_{-,M}^*]^T$ include the positive and conjugate negative sequence phasors, respectively, as defined in (6) and (7). In particular, for a perfectly balanced system, $\mathbf{c}_- = \mathbf{0}$ and, thus, the model in (11) is reduced to

$$\mathbf{z}[n] = e^{j\gamma \frac{\omega_0 + \Delta}{\omega_0} n} \mathbf{B}\mathbf{c}_+ + \mathbf{w}[n], \quad n = 0, \dots, N - 1. \quad (12)$$

If some of the buses are unbalanced, then only the elements of the vector \mathbf{c}_- that are related to the balanced buses are equal to zero. In this case, the measurement model in (11) can be reformulated accordingly, as shown in the next section. We consider the following problem: given the observation vector, $\mathbf{z}[n]$, $n = 0, \dots, N - 1$, determine the imbalance condition of each of the M buses in the network. Thus, there are in total $P = 2^M$ different possible events, which correspond to all the

possible subsets of unbalanced buses from the M buses in the network.

III. NETWORKED IDENTIFICATION VIA THE MDL APPROACH

In this section, we formulate our problem as a model selection problem with multiple hypotheses, where the hypotheses correspond to the number and location of unbalanced buses. Model selection refers to finding the most suitable choice of the model from a set of candidates that provides the “best” description of the observations.

A. The hypothesis-testing problem

The task of identifying the subset of unbalanced buses is equivalent to finding the support of the indices of nonzero elements of \mathbf{c}_- . This can be done by selecting from amongst the multiple hypotheses:

$$\mathcal{H}_i : \mathbf{z}[n] = e^{j\gamma \frac{\omega_0 + \Delta}{\omega_0} n} \mathbf{B} \mathbf{c}_+ + e^{-j\gamma \frac{\omega_0 + \Delta}{\omega_0} n} \mathbf{B}^{(i)} \mathbf{c}_- + \mathbf{w}[n], \quad (13)$$

for $i = 0, 1, \dots, P$ and $n = 0, \dots, N-1$, where $\mathbf{B}^{(i)} \triangleq \mathbf{B}_{\mathcal{S}_i}$, $\mathbf{c}_-^{(i)} \triangleq [\mathbf{c}_-]_{\mathcal{S}_i}$, and \mathcal{S}_i is the subset of nonzero indices of \mathbf{c}_- under hypothesis i . For example, under hypothesis \mathcal{H}_0 , the system is fully balanced, \mathcal{S}_0 is an empty set, and the measurement model is given by (12).

The nested composite multiple hypothesis-testing problem in (13) can be approximated by using the asymptotically-consistent MDL model selection criterion [39], [40], which is widely employed in signal and array processing. The MDL method chooses the hypothesis \mathcal{H}_i which minimizes the sum of two terms: the likelihood term for data encoding, evaluated at the ML points, and a penalty function that inhibits the number of free parameters of the model from becoming very large. For our model, the MDL term is

$$T_{\text{MDL}}^{(i)} = -L(\hat{\mathbf{c}}_+^{(i)}, \hat{\mathbf{c}}_-^{(i)}) + \frac{n^{(i)}}{2} \log N, \quad i = 1, \dots, P, \quad (14)$$

where $\hat{\mathbf{c}}_+^{(i)}$ and $\hat{\mathbf{c}}_-^{(i)}$ are the ML estimates of \mathbf{c}_+ and \mathbf{c}_- , respectively, under the i th hypothesis. Based on (13), the measurement log-likelihood function under each hypothesis, i , is given by:

$$L(\mathbf{c}_+, \mathbf{c}_-^{(i)}) = \text{const} - \frac{1}{\sigma^2} \times \sum_{n=0}^{N-1} \left\| \mathbf{z}[n] - e^{j\gamma \frac{\omega_0 + \Delta}{\omega_0} n} \mathbf{B} \mathbf{c}_+ - e^{-j\gamma \frac{\omega_0 + \Delta}{\omega_0} n} \mathbf{B}^{(i)} \mathbf{c}_-^{(i)} \right\|_2^2, \quad (15)$$

$i = 1, \dots, P$, where “const” is a constant term which is independent of the unknown vectors, \mathbf{c}_+ and $\mathbf{c}_-^{(i)}$, and of the hypothesis \mathcal{H}_i . The number of free (real) unknown parameters, $n^{(i)}$, is equal to the dimension of the complex vectors \mathbf{c}_+ and \mathbf{c}_- . That is, under the i th hypothesis

$$n^{(i)} = 2M + 2|\mathcal{S}_i|, \quad (16)$$

where $|\mathcal{S}_i|$ is the number of unbalanced buses under hypothesis i , i.e. the length of $[\mathbf{c}_-]_{\mathcal{S}_i}$.

B. Networked ML state estimation

In order to implement the MDL rule from (14), we first develop the ML estimators under each hypothesis.

By equating the derivative of (15) with respect to \mathbf{c}_+ to zero, one obtains (e.g. Chapter 4 in [48] and [49])

$$\hat{\mathbf{c}}_+^{(i)} = \mathbf{B}^\dagger \left(\mathbf{z}_+ - \eta \mathbf{B}^{(i)} \hat{\mathbf{c}}_-^{(i)} \right), \quad (17)$$

where

$$\mathbf{z}_+ \triangleq \frac{1}{N} \sum_{n=0}^{N-1} e^{-j\gamma \frac{\omega_0 + \Delta}{\omega_0} n} \mathbf{z}[n], \quad \eta \triangleq \frac{1}{N} \sum_{n=0}^{N-1} e^{-j2\gamma \frac{\omega_0 + \Delta}{\omega_0} n}.$$

Similarly, by equating the derivative of (15) with respect to $\mathbf{c}_-^{(i)}$ to zero, we have

$$\hat{\mathbf{c}}_-^{(i)} = \left(\mathbf{B}^{(i)} \right)^\dagger \left(\mathbf{z}_- - \eta^* \mathbf{B} \hat{\mathbf{c}}_+^{(i)} \right), \quad (18)$$

where

$$\mathbf{z}_- \triangleq \frac{1}{N} \sum_{n=0}^{N-1} e^{j\gamma \frac{\omega_0 + \Delta}{\omega_0} n} \mathbf{z}[n].$$

In particular, for the perfectly balanced hypothesis \mathcal{H}_0 , as described in (12), the ML estimator from (17) and (18) are reduced to $\hat{\mathbf{c}}_+^{(i=0)} = \mathbf{B}^\dagger \mathbf{z}_+$ and $\hat{\mathbf{c}}_-^{(i=0)} = 0$, which coincides with existing results on the ML estimator for balanced systems (e.g. [1]).

Substituting (17) in (18) results in

$$\hat{\mathbf{c}}_-^{(i)} = \left(\mathbf{B}^{(i)} \right)^\dagger \left(\mathbf{z}_- - \eta^* \mathbf{B} \mathbf{B}^\dagger \left(\mathbf{z}_+ - \eta \mathbf{B}^{(i)} \hat{\mathbf{c}}_-^{(i)} \right) \right). \quad (19)$$

Therefore, assuming¹ $\eta \neq 1$ and using the fact that $\left(\mathbf{B}^{(i)} \right)^\dagger \mathbf{B} \mathbf{B}^\dagger \mathbf{B}^{(i)} = \mathbf{I}_{|\mathcal{S}_i|}$, (19) implies that

$$\hat{\mathbf{c}}_-^{(i)} = \frac{1}{1 - |\eta|^2} \left(\mathbf{B}^{(i)} \right)^\dagger \left(\mathbf{z}_- - \eta^* \mathbf{B} \mathbf{B}^\dagger \mathbf{z}_+ \right). \quad (20)$$

Plugging (20) into (17) and using $\mathbf{B}^{(i)} \left(\mathbf{B}^{(i)} \right)^\dagger \mathbf{B} \mathbf{B}^\dagger = \mathbf{B}^{(i)} \left(\mathbf{B}^{(i)} \right)^\dagger$, results in

$$\hat{\mathbf{c}}_+^{(i)} = \frac{1}{1 - |\eta|^2} \mathbf{B}^\dagger \left(\mathbf{G}_i \mathbf{z}_+ - \eta \mathbf{B}^{(i)} \left(\mathbf{B}^{(i)} \right)^\dagger \mathbf{z}_- \right), \quad (21)$$

where $\mathbf{G}_i \triangleq (1 - |\eta|^2) \mathbf{I} + |\eta|^2 \mathbf{B}^{(i)} \left(\mathbf{B}^{(i)} \right)^\dagger$.

The estimators in (20) and (21) are functions of the frequency deviation, Δ . If Δ is unknown, then by equating the derivative of (15) with respect to Δ to zero, we can obtain its ML estimator. For real-time applications, this estimate, which is based on searching the parameter space, can be replaced by low-complexity frequency estimation methods [1], [11], [51]. In particular, in this paper we use the estimate [1]:

$$\hat{\Delta} = \frac{\omega_0}{NM\gamma} \sum_{m=1}^M \sum_{n=0}^{N-2} \angle(v_{+,m}[n+1]) - \angle(v_{+,m}[n]), \quad (22)$$

where $\angle(\cdot)$ denotes the angle of its argument. Then, the state estimators in (20) and (21) are updated accordingly. In this case, i.e. unknown frequency, the number of free parameters from (16), n_i , must be incremented by one.

¹Typical frequency-deviation values in power systems satisfy $|\Delta| \leq 0.1\pi$ [50]. Thus, it can be verified that $|\eta| \ll 1$ for $N > 1$.

C. The MDL method

Substituting the ML estimator from (17) in (15), we obtain

$$L(\hat{\mathbf{c}}_+, \hat{\mathbf{c}}_-^{(i)}) = -\frac{1}{\sigma^2} \sum_{n=0}^{N-1} \left\| \mathbf{z}[n] - e^{j\gamma \frac{\omega_0 + \Delta}{\omega_0} n} \mathbf{B} \mathbf{B}^\dagger \mathbf{z}_+ \right\|_2^2 + \frac{N(1 - |\eta|^2)}{\sigma^2} \left\| \mathbf{B}^{(i)} \hat{\mathbf{c}}_-^{(i)} \right\|_2^2, \quad (23)$$

where we used the fact that $(\mathbf{B}^{(i)})^H \mathbf{B} \mathbf{B}^\dagger \mathbf{B}^{(i)} = (\mathbf{B}^{(i)})^H \mathbf{B}^{(i)}$. Removing the terms that are independent of the hypothesis and substituting (16) and (23) into (14), the MDL criterion for selection of the set of unbalanced buses is based on choosing the hypothesis which maximizes

$$T_i^{(\text{MDL})} = \frac{N(1 - |\eta|^2)}{\sigma^2} \left\| \mathbf{B}^{(i)} \hat{\mathbf{c}}_-^{(i)} \right\|_2^2 - |\mathcal{S}_i| \log N = \frac{N}{\sigma^2(1 - |\eta|^2)} \left\| \mathbf{B}^{(i)} (\mathbf{B}^{(i)})^\dagger (\mathbf{z}_- - \eta^* \mathbf{z}_+) \right\|_2^2 - |\mathcal{S}_i| \log N, \quad (24)$$

for all $i = 1, \dots, P$, where the last equality is obtained by substituting (20) and using $\mathbf{B}^{(i)} (\mathbf{B}^{(i)})^\dagger \mathbf{B} \mathbf{B}^\dagger = \mathbf{B}^{(i)} (\mathbf{B}^{(i)})^\dagger$. It can be seen that the positive sequence phasor ML estimator is absent from the MDL expression in (24). This result stems from the fact that the positive sequence appears under any hypothesis and, hence, cannot be used to distinguish between hypotheses. Therefore, the MDL criterion in (24) can be interpreted as a detector of the presence of the negative sequence phasors, with a penalty function that inhibits the number of unbalanced buses, $|\mathcal{S}_i|$, from becoming very large. The MDL approach is summarized in Algorithm 1.

For the special case of voltage measurements only, $K = M$, $\mathbf{B} = \mathbf{I}_M$ and, thus, the state estimators from (20) and the MDL from (24) are reduced to

$$\hat{\mathbf{c}}_-^{(i)} = \frac{1}{1 - |\eta|^2} ([\mathbf{z}_-]_{\mathcal{S}_i} - \eta^* [\mathbf{z}_+]_{\mathcal{S}_i}) \quad (25)$$

and

$$T_i^{(\text{MDL})} = \frac{N}{\sigma^2(1 - |\eta|^2)} \left\| [\mathbf{z}_-]_{\mathcal{S}_i} - \eta^* [\mathbf{z}_+]_{\mathcal{S}_i} \right\|_2^2 - |\mathcal{S}_i| \log N, \quad (26)$$

respectively.

IV. LOW-COMPLEXITY IDENTIFICATION METHODS

Detecting multiple simultaneous imbalances in power networks using the MDL approach from Algorithm 1 is time-consuming, due to the number of hypotheses that grow exponentially with the network size. In particular, the MDL approach requires an exhaustive search and evaluation of $T_i^{(\text{MDL})}$ over all candidate subsets of unbalanced buses. In this section we develop two low-complexity identification methods. The first is a decentralized, local approach, in which the imbalance detection and state estimation are performed separately at each bus. The second is a computationally-efficient CS technique that is developed by using the sparsity of the negative sequence phasor vector, \mathbf{c}_- .

Algorithm 1: MDL-based networked unbalanced bus identification and state estimation

Input: Observation vectors $\mathbf{z}[n]$, $n = 0, \dots, N - 1$, nominal frequency ω_0 , and system topology \mathbf{B} .
Output: Subset of unbalanced buses, $\mathcal{S}^{(i_{\text{opt}})}$, and state estimators, $\hat{\mathbf{c}}_-^{(i_{\text{opt}})}$ and $\hat{\mathbf{c}}_+^{(i_{\text{opt}})}$.
for $i = 0, 1, \dots, P$ **do**
 1) Estimate the negative-sequence vector, $\hat{\mathbf{c}}_i$, via (20)
 2) Substitute $|\mathcal{S}_i|$ and $\hat{\mathbf{c}}_i$ in (24) to obtain the MDL statistic for the i th hypothesis, $T_i^{(\text{MDL})}$
end
Select the optimal subset, $\mathcal{S}^{(i_{\text{opt}})}$, by:

$$i_{\text{opt}} = \arg \max_{i=0,1,\dots,P} T_i^{(\text{MDL})}. \quad (27)$$

Compute the state estimators from (20) and (21) for the selected subset of unbalanced buses, $\mathcal{S}^{(i_{\text{opt}})}$:

$$\hat{\mathbf{c}}_+^{(i_{\text{opt}})} = \frac{1}{1 - |\eta|^2} \mathbf{B}^\dagger (\mathbf{G}_{i_{\text{opt}}} \mathbf{z}_+ - \eta \mathbf{B}^{(i_{\text{opt}})} (\mathbf{B}^{(i_{\text{opt}})})^\dagger \mathbf{z}_-)$$

$$\hat{\mathbf{c}}_-^{(i_{\text{opt}})} = \frac{1}{1 - |\eta|^2} (\mathbf{B}^{(i_{\text{opt}})})^\dagger (\mathbf{z}_- - \eta^* \mathbf{B} \mathbf{B}^\dagger \mathbf{z}_+),$$

where \mathbf{z}_+ , \mathbf{z}_- , η , and \mathbf{G}_i are defined in Subsection III-B.

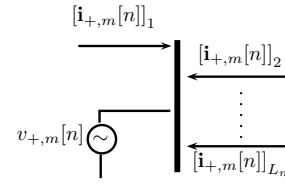


Fig. 2. Single PMU model at the m th bus with a single voltage and L_m currents measurements.

A. Local detection

In this subsection, the MDL approach is performed separately at each bus. Thus, the proposed local MDL approach has the advantage that it can be implemented for distributed detection, without using the central information. At the m th bus, the PMU measures synchronously the voltage at the bus and the current flows on lines incident to this bus, as presented schematically in Fig. 2. Based on the local observations, $\mathbf{z}_m[n]$, $n = 0, \dots, N - 1$, from the m th bus, we seek to identify all the observable buses. Therefore, in this case, $K = 1$, $\mathbf{z}_{+,m} \triangleq \frac{1}{N} \sum_{n=0}^{N-1} e^{-j\gamma \frac{\omega_0 + \Delta}{\omega_0} n} \mathbf{z}_m[n]$, $\mathbf{z}_{-,m} \triangleq \frac{1}{N} \sum_{n=0}^{N-1} e^{j\gamma \frac{\omega_0 + \Delta}{\omega_0} n} \mathbf{z}_m[n]$, and the local system submatrix is $\mathbf{B} = \begin{bmatrix} \mathbf{e}_m^T \\ \mathbf{Y}_m \end{bmatrix}$, in which \mathbf{e}_m is a zeros vector with one at the m row and \mathbf{Y}_m relates the current phasors to the state vector at the m th bus. By using these values in Algorithm 1, we obtain the local MDL approach.

In particular, if only voltage measurements are available, then it can be shown that the local MDL approach reduces to a local detector, which declares that the m th bus is unbalanced when

$$T_m^{(\text{local})} \triangleq \frac{N}{\sigma^2} |z_{-,m} - \eta^* z_{+,m}|^2 > \log N(1 - |\eta|^2). \quad (28)$$

The local MDL test, $T_m^{(\text{local})}$, from (28) provides the same decision rule as the GLRT for a binary hypothesis-testing

problem with a fixed threshold. The proposed GLRT approach in (28) is the first method for local imbalances detection that is based solely on the positive sequence. In addition, by comparing (26) and (28), it can be verified that the local MDL coincides with the centralized MDL where only voltage measurements are available. Therefore, in this case, we can obtain the networked performance by applying a detector at each bus separately.

B. The POMP method

In order to use CS techniques [31], we first observe that in the measurement model from (11) the negative-sequence state vector, \mathbf{c}_- , is a sparse vector. That is, \mathbf{c}_- has only a few nonzero elements that are related to the unbalanced buses. Thus, the low-complexity POMP method from [49] may be exploited to identify the support of \mathbf{c}_- , as well as greedy CS algorithms with partial known support (e.g. [52]–[54]). The POMP concept is a low-complexity CS technique for estimating two vectors in a linear Gaussian model, where one of the unknown vectors is subject to a sparsity constraint. Here we adopt the POMP method to the specific model in (11).

First, we notice that, similarly to the derivation of (20) and (23), for a given sparsity level, s , the ML estimator of \mathbf{c}_- is given by

$$\hat{\mathbf{c}}_- = \arg \min_{\mathbf{c}_-, s.t. \|\mathbf{c}_-\|_0=s} \left\| \frac{\mathbf{z}_- - \eta^* \mathbf{B} \mathbf{B}^\dagger \mathbf{z}_+}{1 - |\eta|^2} - \mathbf{B} \mathbf{c}_- \right\|_2^2.$$

Therefore, based on our work from [49], the POMP algorithm can be applied on our problem. POMP for our model consists of two stages:

- 1) **Imbalance identification:** The OMP method iteratively finds the locations of the unbalanced buses, i.e. the support set \mathcal{S} of the vector \mathbf{c}_- , by using the projected measurements $\tilde{\mathbf{z}} \triangleq \frac{1}{1-|\eta|^2} (\mathbf{z}_- - \eta^* \mathbf{B} \mathbf{B}^\dagger \mathbf{z}_+)$. At each iteration, the OMP algorithm proceeds by finding the column of the matrix \mathbf{B} that correlates most closely to the current residual, $\mathbf{r}^{(k)}$, where k is the iteration index. The residual $\mathbf{r}^{(k)}$ is obtained by subtracting the contribution of the current estimate of \mathbf{c}_- from the projected measurements.
- 2) **State estimation:** The final estimation of the support set, $\hat{\mathcal{S}}$, is used to calculate $\mathbf{B}^{(i)} = \mathbf{B}_{\hat{\mathcal{S}}}$. Then, the state vectors, $[\mathbf{c}_-]_{\hat{\mathcal{S}}}$ and $\mathbf{c}_+^{(i)}$, are estimated by substituting $\mathbf{B}^{(i)} = \mathbf{B}_{\hat{\mathcal{S}}}$ in (20) and (21), respectively.

The proposed POMP method is described in Algorithm 2.

C. Conditions for solution existence

Since we assumed that the system is perfectly observable by the installed PMUs, the matrix \mathbf{B} is a full column rank matrix and $K + L \geq M$. In addition, the state estimators in (20) and (21) are based on the assumption that $N > 1$ in order to have $\eta \neq 1$. In general, the unknown phasor vectors, \mathbf{c}_+ and \mathbf{c}_- , have $2M$ unknown complex parameters. Therefore, in order to have a unique solution, we require that our observations satisfy $N(K + L) \geq 2M$. Together with the observability assumption, it can be verified that $N \geq 2$ time samples is a sufficient condition for a unique solution. Since the POMP approach requires estimation of only $M + |\mathcal{S}|$ unknown parameters,

Algorithm 2: POMP method for unbalanced bus identification and state estimation

Input: Observation vector $\mathbf{z}[n]$, $n = 0, \dots, N - 1$, nominal frequency ω_0 , system topology \mathbf{B} , and threshold for the breaking point, τ .
Output: Subset of unbalanced buses, $\mathcal{S}^{(k)}$, and state estimators, $\hat{\mathbf{c}}_+^{(\text{POMP})}$ and $\hat{\mathbf{c}}_-^{(\text{POMP})}$.

Initialization

Fix $k = 0$; Set the temporary solution, residual, and support to:

$$\hat{\mathbf{c}}_-^{(k)} = \mathbf{0}, \quad \mathbf{r}^{(k)} = \frac{1}{1 - |\eta|^2} (\mathbf{z}_- - \eta^* \mathbf{B} \mathbf{B}^\dagger \mathbf{z}_+), \quad \mathcal{S}^{(k)} = \emptyset.$$

while $\|\mathbf{r}^{(k)}\|_2^2 > \tau$ **do**

 Increment k and apply:

- 1) Update support: Find l_0 such that

$$l_0 = \arg \max_{l \in \{1, \dots, M\}} \frac{|\mathbf{b}_l^H \mathbf{r}^{(k-1)}|^2}{\mathbf{b}_l^H \mathbf{b}_l},$$

 where \mathbf{b}_l is the l th column of the matrix \mathbf{B} , and update $\mathcal{S}^{(k)} = \mathcal{S}^{(k-1)} \cup l_0$ accordingly.

- 2) Update solution: Compute the state estimators from (20) for the current subset of unbalanced buses, $\mathcal{S}^{(k)}$:

$$[\hat{\mathbf{c}}_-^{(k)}]_{\mathcal{S}^{(k)}} = \frac{1}{1 - |\eta|^2} ([\mathbf{B}]_{\mathcal{S}^{(k)}})^\dagger (\mathbf{z}_- - \eta^* \mathbf{B} \mathbf{B}^\dagger \mathbf{z}_+)$$

- 3) Update residual: Compute

$$\mathbf{r}^{(k)} = \frac{1}{1 - |\eta|^2} (\mathbf{z}_- - \eta^* \mathbf{B} \mathbf{B}^\dagger \mathbf{z}_+) - \mathbf{B}_{\mathcal{S}^{(k)}} [\hat{\mathbf{c}}_-^{(k)}]_{\mathcal{S}^{(k)}}$$

end

 Compute $\tilde{\mathbf{G}} \triangleq (1 - |\eta|^2) \mathbf{I} + |\eta|^2 \mathbf{B}_{\hat{\mathcal{S}}} (\mathbf{B}_{\hat{\mathcal{S}}})^\dagger$.

 Compute the state estimators:

$$\hat{\mathbf{c}}_+^{(\text{POMP})} = \frac{1}{1 - |\eta|^2} \mathbf{B}^\dagger (\tilde{\mathbf{G}} \mathbf{z}_+ - \eta \mathbf{B}_{\hat{\mathcal{S}}} \mathbf{B}_{\hat{\mathcal{S}}}^\dagger \mathbf{z}_-) \quad (29)$$

$$[\hat{\mathbf{c}}_-^{(\text{POMP})}]_{\hat{\mathcal{S}}} = \frac{1}{1 - |\eta|^2} \mathbf{B}_{\hat{\mathcal{S}}}^\dagger (\mathbf{z}_- - \eta^* \mathbf{B} \mathbf{B}^\dagger \mathbf{z}_+), \quad (30)$$

 where \mathbf{z}_+ , \mathbf{z}_- and η are defined in Subsection III-B.

as well as identification of the support set, where $|\mathcal{S}|$ is the number of unbalanced buses, then less measurements and/or less PMUs are required. A deeper discussion for the general case, in terms of CS bounds, can be found in [55].

D. Extension to three-phase data

In current power systems, the PMUs transmits only the positive sequence, due to communication bandwidth and processing cost limitations. In the future, wide area monitoring systems may be configured for three-phase measurements. The methods proposed herein can be readily extended to the three-phase measurement case, as we now described.

Similar to (5), by substituting (1)-(3) in (9), we obtain

$$v_{-,m}[n] = e^{j\gamma \frac{\omega_0 + \Delta}{\omega_0} n} C_{-,m} + e^{-j\gamma \frac{\omega_0 + \Delta}{\omega_0} n} C_{+,m}^*, \quad (31)$$

for any $n = 0, \dots, N - 1$ and any bus $m = 1, \dots, M$. Following (11), the model of the negative sequence at the control center is given by

$$\mathbf{y}^*[n] = e^{j\gamma \frac{\omega_0 + \Delta}{\omega_0} n} \mathbf{B}^* \mathbf{c}_+ + e^{-j\gamma \frac{\omega_0 + \Delta}{\omega_0} n} \mathbf{B}^* \mathbf{c}_- + \mathbf{w}_-[n], \quad (32)$$

where $\mathbf{w}_-[n]$ is the networked negative-sequence complex circularly symmetric Gaussian noise at time n , which is assumed to be uncorrelated with $\mathbf{w}[n]$, $n = 0, \dots, N - 1$.

If both the negative and positive sequences are available, then the joint measurement model that merges (11) and (32) is given by

$$\tilde{\mathbf{z}}[n] = e^{j\gamma \frac{\omega_0 + \Delta}{\omega_0} n} \tilde{\mathbf{B}} \mathbf{c}_+ + e^{-j\gamma \frac{\omega_0 + \Delta}{\omega_0} n} \tilde{\mathbf{B}} \mathbf{c}_- + \mathbf{w}_-[n], \quad (33)$$

where $\tilde{\mathbf{z}}[n] \triangleq [\mathbf{z}[n]^T, \mathbf{y}^H[n]]^T$ and $\tilde{\mathbf{w}}[n] \triangleq [\mathbf{w}[n]^T, \mathbf{w}_-^T[n]]^T$, $n = 0, \dots, N - 1$, and $\tilde{\mathbf{B}} \triangleq \begin{bmatrix} \mathbf{B} \\ \mathbf{B}^* \end{bmatrix}$. Since the model in (33) is identical to that in (11), the proposed MDL, local MDL, and POMP can be implemented for the two-phase data by replacing the measurement vectors $\mathbf{z}[n]$ with $\tilde{\mathbf{z}}[n]$ for any $n = 0, \dots, N - 1$, and by replacing the topology matrix \mathbf{B} with $\tilde{\mathbf{B}}$.

In a similar fashion, the proposed methods can be extended to identify zero-phase imbalance scenarios by using three-phase data and obtaining the associated network measurement model as in (11) and (32).

V. SIMULATIONS

In this section, we compare the performance of five methods in three different networks. The methods are: the VUF [17], [18], which is a local, two-phase based detection method that uses the voltage measurements, the GLRT from [24], which is a local, three-phase based detection method that uses the voltage measurements, and the proposed MDL, local MDL, and POMP methods. The networks are for a small two-port π -model network, the IEEE 14-bus, and IEEE 118-bus. The MDL method from Algorithm 1 is applicable only for the first example, due to its computational complexity. The centralized POMP method is implemented with a threshold proportional to $\tau = \|\mathbf{B}\|_2 \frac{\sigma^2}{N}$. The commonly-used VUF statistic is defined as the voltage magnitude ratio of the negative to the positive sequences. In the following simulations, the VUF at the m th bus is defined as

$$T_{\text{VUF},m} = \frac{\sum_{n=0}^{N-1} |v_{-,m}[n]|}{\sum_{n=0}^{N-1} |v_{+,m}[n]|}.$$

For an unbalanced bus, $T_{\text{VUF},m}$ should be close to 1. Therefore, in the following simulations the decision of the VUF detector is based on comparing $|T_{\text{VUF},m} - 1|$ with a threshold. In all simulations, we assume a nominal grid frequency of $\omega_0 = 2\pi \cdot 60$ and an unknown frequency deviation of $\Delta = 0.2\pi$, which is estimated via (22). The performance is evaluated using 10,000 Monte-Carlo simulations.

A. Two-port π -model

We assume the two-port π -model (see e.g. [8] and p. 151 in [1]). We consider two PMUs, one at each end of the transmission line, with a sampling rate of $N = 48$ samples

per cycle of ω_0 . The measurement equation is given by (10), where $\mathbf{v}_+[n] = [v_{1,+}[n], v_{2,+}[n]]^T$ and

$$\mathbf{B} = \begin{bmatrix} 1 & 0 \\ 0 & 1 \\ y_{12} + y_{10} & -y_{12} \\ -y_{12} & y_{20} \end{bmatrix},$$

in which $y_{12}, y_{10}, y_{20}, y_{11}$ represent the corresponding positive sequence series admittances. In this case, there are $P = 4$ hypotheses with balanced/unbalanced conditions for each bus.

A single-phase voltage magnitude imbalance is implemented in bus 2 by setting the parameters as defined in Table I, where the voltage magnitudes are considered to be per unit (p.u.). The admittance parameters are set to $y_{12} = 0.1$, $y_{10} = 0.5$, and $y_{20} = y_{12}$. In Fig 3, the probability of

Bus	Voltage magnitudes	Voltage phases
Bus 1	$V_a = V_b = V_c = 1$	$(\varphi_a, \varphi_b, \varphi_c) = (\frac{\pi}{4}, \frac{\pi}{4} - \frac{2\pi}{3}, \frac{\pi}{4} + \frac{2\pi}{3})$
Bus 2	$V_a = V_c = 1.25, V_b = \beta V_a, \beta > 1$	$(\varphi_a, \varphi_b, \varphi_c) = (-\frac{\pi}{4}, -\frac{\pi}{4} - \frac{2\pi}{3}, -\frac{\pi}{4} + \frac{2\pi}{3})$

TABLE I
EXAMPLE 1 (TWO-PORT π -MODEL): SIMULATION PARAMETERS

error of the different approaches is presented versus β for a noise variance of $\sigma^2 = -5,0\text{dB}$ and $N = 48$. The probability of error is the total probability that the methods incorrectly detected that bus 2 is balanced and/or that bus 1 is unbalanced. The performance of the VUF method in this case is significantly lower than the other methods and their associated probability of error converges to zero only for $\beta > 100$. Hence, for the sake of clarity of Fig. 3, the VUF performance does not depicted. It can be seen that for all the methods the probability of error decreases as the noise variance decreases and as β increases, i.e. for stronger voltage imbalance. While the GLRT method [24] performs well in the low-noise regime, it progressively falls behind all other techniques as the variance of the noise increases. The MDL approach has lower probability of error than the other methods for any signal-to-noise ratio (SNR). The performance of the POMP method is close to that of the MDL approach and depends on the choice of the threshold parameter, τ , from Algorithm 2.

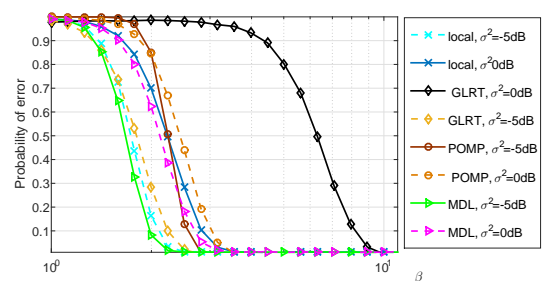


Fig. 3. Two-port π -model: Probability of error for two-port π -model with $\sigma^2 = -5,0\text{dB}$, $N = 48$, and single-phase voltage magnitude imbalance at bus 2.

B. Case study: Loading imbalances

In this subsection, we study loading imbalances in the network model for the IEEE 14-bus system, as shown in Fig. 1, where the system parameters, such as branch impedances, are

taken from [56]. The PMUs are located at buses 2, 6, 7, 9 and measure bus voltages and currents in lines connected to these buses, which results in an observable system [44]. This setting results in a total of 18 sensor measurements and 14 unknown positive sequence phasors. At each Monte Carlo run, PMU measurements were generated as an independent identically distributed (i.i.d.) Gaussian random vector with the mean equal to the operating point given in the IEEE 14-bus data [56] and covariance matrix $\sigma^2 \mathbf{I}_{18}$. Similar to [2], loading imbalances are found at the load buses 4, 5 and 9. To generate single-phase imbalances, we multiply the amplitude of phase c load by $\beta > 1$ at the unbalanced buses. The local MDL method is performed based on the single PMU located at bus 7. Thus, the local method is only able to identify the imbalance condition of buses 4, 7, 8 and 9. The VUF and GLRT methods [24] are only based on voltage measurements; thus, they are only able to identify the imbalance condition of buses 2, 6, 7, 9.

Figure 4 shows the Receiver Operating Characteristic (ROC) curves of the VUF, GLRT, local MDL, and POMP methods for the detection of imbalance at bus 9 for two scenarios: 1) $\beta = 3.75$ and $N = 24$; and 2) $\beta = 1.1$ and $N = 12$. It can be seen that the POMP and local MDL approaches significantly outperform the VUF and GLRT, where for small values of β the imbalance is undetectable by the VUF and GLRT. In Fig. 5, the probability of detection of all the unbalanced buses, 4, 5 and 9, is presented versus β for $N = 10$ and $\text{SNR} = 10\text{db}$, where $\text{SNR} \triangleq \frac{N}{\sigma^2}$. The probability of false alarm, is around 5% for all methods. It can be seen that the detection probability is higher for the POMP than for the local MDL method at buses 4 and 9, and than for the VUF and GLRT methods at bus 9. The reason is that the local MDL approach is based only on the local single-bus PMU measurements, which results in lower accuracy compared with centralized approaches. The VUF and GLRT use only voltage measurements, which results in a lower detection probability compared with the single-phase approaches, POMP and local MDL. Therefore, it can be concluded that the use of both current and voltage single-phase measurements is better than the use of two-/three-phase voltage-only data. Moreover, imbalance at bus 5 is undetectable by the local methods, since this bus is unobservable by the PMU located at buses 7 nor 9. That is, the POMP approach is the only method that achieves full observability of the system.

C. Case study: Loading imbalances in large-scale networks

The purpose of this experiment is to investigate the performance of the proposed algorithm when applied to large systems. In particular, we study loading imbalances in the IEEE 118-bus system, where the system parameters are taken from [56] and the PMUs are located according to the “base case state” outlined in Table V in [57], which results in an observable system [44], [57]. This setting results in a total of 133 sensor measurements and 118 unknown positive sequence phasors. At each Monte Carlo run, PMU measurements were generated as an i.i.d. Gaussian random vector with the mean equal to the operating point given in the IEEE 118-bus data [56] and the covariance matrix $\sigma^2 \mathbf{I}_{133}$. Loading single-phase imbalances are implemented at load buses, that are randomly chosen to be 3, 9, 33, 39, 51, 57, 75, 93, 96, 98, with $\beta > 1$ at the unbalanced buses. The local MDL method is performed,

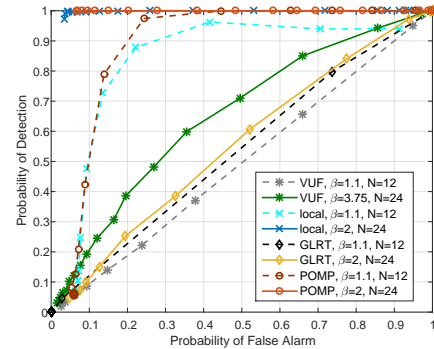


Fig. 4. Loading imbalances for IEEE 14-bus system: The ROC curves of VUF, GLRT, local MDL, and POMP for detection of single-phase magnitude imbalance at bus 9, with 1) $\beta = 3.75$ and $N = 24$ (solid line); and 2) $\beta = 1.1$ and $N = 12$ (dashed line). The local method is based on the single PMU located at bus 7.

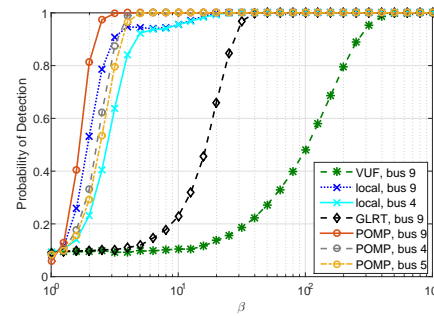


Fig. 5. Loading imbalances for IEEE 14-bus system: Probability of detection for $N = 10$ and $\text{SNR} = 10\text{db}$, single-phase magnitude imbalance at buses 4, 5 and 9, and PMUs at buses 2, 6, 7, 9. The local method is based on the single PMU located at bus 7 and the VUF and GLRT on bus 9 voltage three-phase measurements.

based on the single PMU located at bus 9. Thus, the local method is only able to identify the imbalance condition of buses 8, 9 and 10.

Figure 6 shows the ROC curves of the VUF, GLRT, local MDL, and POMP methods, where bus 9 is unbalanced for two scenarios: 1) $\beta = 3.75$ and $N = 24$ (solid line); and 2) $\beta = 1.1$ and $N = 12$ (dashed line). It can be seen that the POMP and local MDL approaches significantly outperform the VUF and the GLRT methods, for which at small values of β the imbalance is undetectable. The behavior of MDL can be explained by the fact that this criterion has been shown to be inconsistent when the variance of the noise tends to zero [58]. In Fig. 5, the probability of detection of the unbalanced buses is presented versus β for $N = 10$. The probability of false alarm, is around 10% for all methods. Evidently, the detection probability is higher for POMP than for the local MDL method at bus 9, and than for the VUF and GLRT at bus 9. This effect is expected to be higher for a larger network. The reason is that the local MDL approach is based only on the local single-bus PMU measurements, which results in lower accuracy compared with centralized approaches.

Comparison between the results of the IEEE 14-bus system in Figs. 4 and 5 and those of the IEEE 118-bus system in Figs. 6 and 7, indicates that the VUF and local MDL techniques have better performance for the smaller 14-bus system, the

GLRT method has better performance for the large 118-bus system, and the POMP algorithm performs well for both the 14-bus and 118-bus systems.

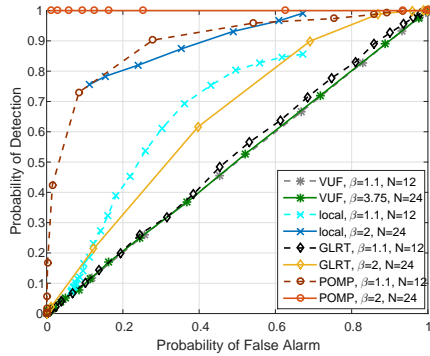


Fig. 6. Loading imbalances for IEEE 118-bus system: The ROC curves of VUF, GLRT, local MDL, and POMP methods for detection of single-phase magnitude imbalance at bus 9, with 1) $\beta = 3.75$ and $N = 24$ (circle); and 2) $\beta = 1.1$ and $N = 12$ (diamond). The local method is based on the single PMU located at bus 9.

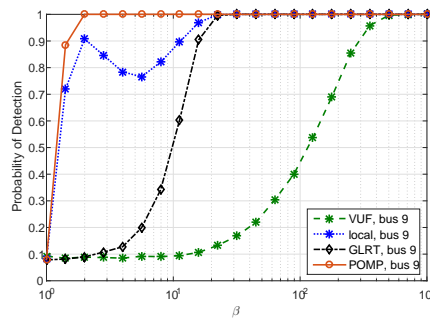


Fig. 7. Loading imbalances for IEEE 118-bus system: Probability of detection for single-phase magnitude imbalance at buses 3, 9, 33, 39, 51, 57, 75, 93, 96, 98 with $N = 10$ and $SNR = 10db$. The local method is based on the single PMU located at bus 9 and the VUF and GLRT on bus 9 voltage three-phase measurements.

The probability of detection of the VUF, GLRT, local MDL, and POMP methods versus the number of unbalanced load buses, which is equivalent to the sparsity level, is presented in Fig. 8 for $SNR = 10db$ and two scenarios: 1) $\beta = 1.1$ and $N = 12$; and 2) $\beta = 3.75$ and $N = 24$. In addition, for the centralized POMP, the following probabilities computed among all the buses in the system are presented:

- $Pr_{correct}$ - the probability of correct decision (balanced/unbalanced bus) for all the 118 buses;
- $Pr_{over\ estimation}$ - the probability to overestimate the number of unbalanced buses in the system.

It can be seen that the *local* detection performance of all methods at bus 9 is independent of the number of unbalanced buses in the system. For POMP, which is the only centralized method that can deal with the entire system, the probability of overestimation decreases and the probability of correct decision decreases as the number of unbalanced buses in the system increases. For $\beta = 3.75$, $N = 24$, and $SNR = 10db$ the probability of correct decision is higher than 0.92 for any number of buses. Thus, we can conclude that the proposed POMP algorithm is scalable.

In order to demonstrate the complexity of POMP for different problem dimensions, the average processing period,

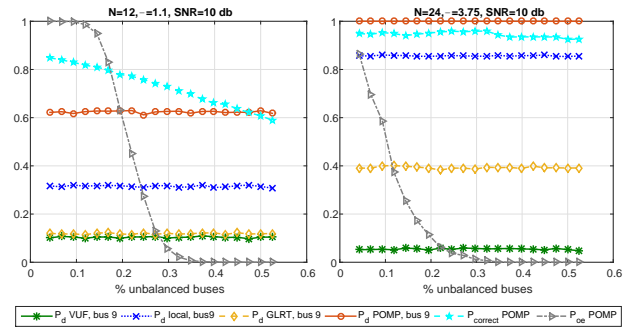


Fig. 8. The probability of detection of the VUF, GLRT, local MDL, and POMP methods and the probabilities of correct decision and the probability of overestimation for POMP versus the number of buses for IEEE 118-bus system with 1) $\beta = 1.1$, $N = 12$, and $SNR = 10db$ (left); and 2) $\beta = 3.75$, $N = 24$, and $SNR = 10db$ (right)

“runtime”, was evaluated by running the algorithm using Matlab on an Intel Core(TM) i7-5820K CPU computer, 3.3 GHz. Figure 9 shows the runtime of the POMP method as a function of the percent of unbalanced load buses in the system for 14-bus and 118-bus systems and $N = 12, 24$ samples. It can be seen that the runtime is higher for the 118-bus system than for the 14-bus system, as expected, but it has the same order. In addition, the runtime increases approximately linearly with the problem dimensions. It should be noted that POMP is the only centralized method that is not restricted to very small problem dimensions.

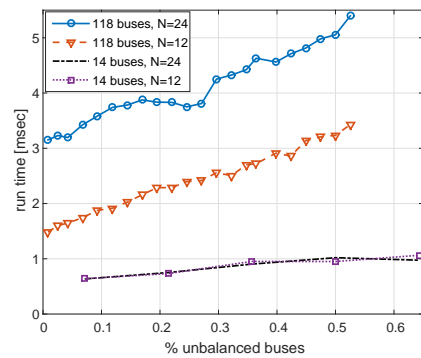


Fig. 9. Runtime of the POMP method versus percent of unbalanced buses in 14-bus and 118-bus systems and $N = 12, 24$ samples.

VI. CONCLUSION

In this paper, we proposed two methods to identify and localize imbalances occurring at any location in the power grid and, simultaneously, estimate the states, based on single-phase PMU measurements. The single-phase data affords low communication and processing costs, compared to three-phase data processing. The proposed MDL and POMP approaches use central information from the entire network, where the POMP method has reduced computational complexity. The difference between the centralized and the distributed implementations is that the former performs the state estimation and imbalance detection steps over the complete data set and, thus, is more accurate, whereas in the latter each bus runs these steps on its own local data. Simulation results confirm that the proposed approaches are feasible and that the centralized detection methods, MDL and POMP, display superior performance,

compared to the local MDL method. For small-scale networks, it is shown that the performance of POMP converges to that of the asymptotically-consistent MDL approach. However, the centralized MDL, which has the lowest probability of error, cannot be implemented on large-scale networks. Thus, the proposed POMP method provides the best performance, in terms of high probability of detection and low runtime for large-scale networks. The local MDL method achieves better performance compared with *local* methods, i.e. GLRT and VUF, and the performance of the local MDL converges to that of the POMP algorithm for high SNR and/or a large number of measurements.

REFERENCES

- [1] A. Phadke and J. Thorp, *Synchronized Phasor Measurements and Their Applications*. New York: Springer Science, 2008.
- [2] S. Zhong and A. Abur, "Effects of nontransposed lines and unbalanced loads on state estimation," in *IEEE Power Engineering Society Winter Meeting*, vol. 2, Jan. 2002, pp. 975–979.
- [3] N. Woolley and J. Milanovic, "Statistical estimation of the source and level of voltage unbalance in distribution networks," *IEEE Trans. Power Delivery*, vol. 27, no. 3, pp. 1450–1460, July 2012.
- [4] S. Urano, T. Yamada, Y. Ooura, Y. Xu, and Y. Yamaguchi, "Development of the high accuracy impedance type fault locator using a mode transformation," in *2005 IEEE/PES Transmission Distribution Conference Exposition: Asia and Pacific*, Aug. 2005, pp. 1–6.
- [5] A. Meliopoulos, B. Fardanesh, and S. Zelingher, "Power system state estimation: modeling error effects and impact on system operation," in *Annual Hawaii International Conference on System Sciences*, Jan. 2001.
- [6] B. Van Tuykom, J. C. Maun, and A. Abur, "Use of phasor measurements and tuned weights for unbalanced system state estimation," in *North American Power Symposium (NAPS), 2010*, Sep. 2010, pp. 1–5.
- [7] A. Gomez-Exposito, A. Abur, A. de la Villa Jaen, and C. Gomez-Quiles, "A multilevel state estimation paradigm for smart grids," *Proceedings of the IEEE*, vol. 99, no. 6, pp. 952–976, June 2011.
- [8] A. Abur and A. Gomez-Exposito, *Power System State Estimation: Theory and Implementation*. Marcel Dekker, 2004.
- [9] F. Schweppe and J. Wildes, "Power system static-state estimation, part I: Exact model," *IEEE Trans. Power Apparatus and Systems*, vol. PAS-89, pp. 120–125, Jan. 1970.
- [10] T. Routtenberg and L. Tong, "Joint frequency and phasor estimation under the KCL constraint," *IEEE Signal Processing Letters*, vol. 20, no. 6, pp. 575–578, June 2013.
- [11] Y. Xia and D. Mandic, "Widely linear adaptive frequency estimation of unbalanced three-phase power systems," *IEEE Trans. Instrumentation and Measurement*, vol. 61, no. 1, pp. 74–83, Jan. 2012.
- [12] Y. Xia, S. Douglas, and D. Mandic, "Adaptive frequency estimation in smart grid applications: Exploiting noncircularity and widely linear adaptive estimators," *IEEE Signal Processing Magazine*, vol. 29, no. 5, pp. 44–54, Sep. 2012.
- [13] T. Routtenberg, Y. Xie, R. M. Willett, and L. Tong, "PMU-based detection of imbalance in three-phase power systems," *IEEE Trans. Power System*, vol. 30, no. 4, pp. 1966–1976, July 2015.
- [14] A. Angioni, C. Muscas, S. Sulis, F. Ponci, and A. Monti, "Impact of heterogeneous measurements in the state estimation of unbalanced distribution networks," in *Instrumentation and Measurement Technology Conference (I2MTC)*, May 2013, pp. 935–939.
- [15] V. Choqueuse, A. Belouchrani, E.-H. El Bouchikhi, and M. El Hachemi Benbouzid, "Estimation of amplitude, phase and unbalance parameters in three-phase systems: Analytical solutions, efficient implementation and performance analysis," *IEEE Trans. Signal Processing*, vol. 62, no. 16, pp. 4064–4076, Aug. 2014.
- [16] F. Alcantara and P. Salmeron, "A new technique for unbalance current and voltage estimation with neural networks," *IEEE Trans. Power Systems*, vol. 20, no. 2, pp. 852–858, May 2005.
- [17] A. Von Jouanne and B. Banerjee, "Assessment of voltage unbalance," *IEEE Trans. Power Delivery*, vol. 16, no. 4, pp. 782–790, Oct. 2001.
- [18] P. Pillay and M. Manyage, "Definitions of voltage unbalance," *IEEE Power Eng. Rev.*, vol. 21, no. 5, pp. 49–51, May 2001.
- [19] J. G. Kim, E. W. Lee, D. J. Lee, and J. H. Lee, "Comparison of voltage unbalance factor by line and phase voltage," in *Electrical Machines and Systems, 2005. ICEMS 2005. Proceedings of the Eighth International Conference on*, vol. 3, Sep. 2005, pp. 1998–2001.
- [20] P. Pillay and P. Hofmann, "Derating of induction motors operating with a combination of unbalanced voltages and over- or undervoltages," in *IEEE Power Engineering Society Winter Meeting, 2001.*, vol. 3, 2001, pp. 1365–1371.
- [21] J. Faiz, H. Ebrahimpour, and P. Pillay, "Influence of unbalanced voltage on the steady-state performance of a three-phase squirrel-cage induction motor," *IEEE Trans. Energy Conversion*, vol. 19, no. 4, pp. 657–662, Dec. 2004.
- [22] N. Tangsunantham and C. Pirak, "Voltage unbalance measurement in three-phase smart meter applied to AMI systems," in *International Conference on Electrical Engineering, Computer, Telecommunications and Information Technology (ECTI-CON)*, May 2013, pp. 1–5.
- [23] J. Wang, N. Zeng, and H. Hao, "Three-phase imbalance prediction: A hazard-based method," in *IEEE International Conference on Power and Renewable Energy (ICPRE)*, Oct. 2016, pp. 226–231.
- [24] M. Sun, S. Demirtas, and Z. Sahinoglu, "Joint voltage and phase unbalance detector for three phase power systems," *IEEE Signal Processing Letters*, vol. 20, no. 1, pp. 11–14, Jan. 2013.
- [25] R. Concepcion, T. Routtenberg, and L. Tong, "Local detection of voltage imbalance in three-phase power systems based on PMU output," in *Innovative Smart Grid Technologies (ISGT)*, Feb. 2015, pp. 1–5.
- [26] T. Routtenberg, R. Concepcion, and L. Tong, "PMU-based detection of voltage imbalances with tolerance constraints," *IEEE Trans. Power Delivery*, vol. 32, no. 1, pp. 484–494, Feb. 2017.
- [27] T. Routtenberg and Y. Xie, "PMU-based online change-point detection of imbalance in three-phase power systems," in *ISGT 2017*, 2016. [Online]. Available: <http://www.ee.bgu.ac.il/%7etirzar/publications.html>
- [28] C. D. Austin, R. L. Moses, J. N. Ash, and E. Ertin, "On the relation between sparse reconstruction and parameter estimation with model order selection," *IEEE Journal of Selected Topics in Signal Processing*, vol. 4, no. 3, pp. 560–570, June 2010.
- [29] S. S. Chen, D. L. Donoho, and M. A. Saunders, "Atomic decomposition by basis pursuit," *SIAM Review*, vol. 43, no. 1, pp. 129–159, 2001.
- [30] J. A. Tropp, "Greed is good: algorithmic results for sparse approximation," *IEEE Trans. Information Theory*, vol. 50, no. 10, pp. 2231–2242, Oct. 2004.
- [31] Y. C. Eldar and G. Kutyniok, *Compressed Sensing: Theory and Applications*, ser. Compressed Sensing: Theory and Applications. Cambridge University Press, 2012.
- [32] Y. C. Eldar, *Sampling Theory: Beyond Bandlimited Systems*, 1st ed. New York, NY, USA: Cambridge University Press, 2015.
- [33] H. Zhu and G. B. Giannakis, "Sparse overcomplete representations for efficient identification of power line outages," *IEEE Trans. Power Systems*, vol. 27, no. 4, pp. 2215–2224, Nov. 2012.
- [34] J. Chen, Y. Zhao, A. Goldsmith, and H. Poor, "Line outage detection in power transmission networks via message passing algorithms," in *Asilomar Conference*, Nov. 2014, pp. 350–354.
- [35] S. Maymon and Y. C. Eldar, "Identification of power line outages," submitted to *IEEE Trans. Signal Processing*.
- [36] S. Kibria, J. Kim, and R. Raich, "Sparse error correction with multiple measurement vectors," in *IEEE Statistical Signal Processing Workshop (SSP)*, June 2016, pp. 1–5.
- [37] W. Xu, M. Wang, J. F. Cai, and A. Tang, "Sparse error correction from nonlinear measurements with applications in bad data detection for power networks," *IEEE Trans. Signal Processing*, vol. 61, no. 24, pp. 6175–6187, Dec. 2013.
- [38] L. Liu, M. Esmalifalak, Q. Ding, V. A. Emesih, and Z. Han, "Detecting false data injection attacks on power grid by sparse optimization," *IEEE Trans. Smart Grid*, vol. 5, no. 2, pp. 612–621, March 2014.
- [39] J. Rissanen, "Modeling by shortest data description," *Automatica*, vol. 14, no. 5, pp. 465–471, Sep. 1978.
- [40] M. Wax and T. Kailath, "Detection of signals by information theoretic criteria," *IEEE Trans. Acoustics, Speech and Signal Processing*, vol. 33, no. 2, pp. 387–392, Apr. 1985.
- [41] D. L. Donoho, Y. Tsaig, I. Drori, and J. L. Starck, "Sparse solution of underdetermined systems of linear equations by stagewise orthogonal matching pursuit," *IEEE Trans. Information Theory*, vol. 58, no. 2, pp. 1094–1121, Feb. 2012.
- [42] T. Routtenberg and L. Tong, "Networked detection of voltage imbalances for three-phase power system," in *IEEE International Symposium on Industrial Electronics (ISIE 2015)*, June 2015, pp. 1345–1350.
- [43] Z. Oubrahim, V. Choqueuse, Y. Amirat, and M. Benbouzid, "Classification of three-phase power disturbances based on model order selection in smart grid applications," in *IECON 2016 - 42nd Annual Conference of the IEEE Industrial Electronics Society*, Oct. 2016, pp. 5143–5148.
- [44] B. Gou, "Generalized integer linear programming formulation for optimal PMU placement," *IEEE Trans. Power Systems*, vol. 23, no. 3, pp. 1099–1104, Aug. 2008.
- [45] A. G. Phadke, J. S. Thorp, and M. G. Adamiak, "A new measurement technique for tracking voltage phasors, local system frequency, and rate

of change of frequency," *IEEE Trans. Power Apparatus and Systems*, vol. PAS-102, no. 5, pp. 1025–1038, May 1983.

- [46] F. Neves, H. Souza, E. Bueno, M. Rizo, F. Bradaschia, and M. Cavalcanti, "A space-vector discrete fourier transform for detecting harmonic sequence components of three-phase signals," in *IEEE Industrial Electronics (IECON)*, Nov. 2009, pp. 3631–3636.
- [47] G. Paap, "Symmetrical components in the time domain and their application to power network calculations," *IEEE Trans. Power Systems*, vol. 15, no. 2, pp. 522–528, May 2000.
- [48] S. M. Kay, *Fundamentals of statistical signal processing: Estimation Theory*. Englewood Cliffs (N.J.): Prentice Hall PTR, 1993, vol. 1.
- [49] T. Routtenberg, Y. C. Eldar, and L. Tong, "Maximum likelihood estimation under partial sparsity constraints," in *ICASSP 2013*, May 2013, pp. 6421–6425.
- [50] P. Top, M. Bell, E. Coyle, and O. Wasynczuk, "Observing the power grid: Working toward a more intelligent, efficient, and reliable smart grid with increasing user visibility," *IEEE Signal Processing Magazine*, vol. 29, no. 5, pp. 24–32, 2012.
- [51] V. Terzija, N. Djuric, and B. Kovacevic, "Voltage phasor and local system frequency estimation using Newton type algorithm," *IEEE Trans. Power Delivery*, vol. 9, no. 3, pp. 1368–1374, July 1994.
- [52] R. E. Carrillo, L. F. Polania, and K. E. Barner, "Iterative algorithms for compressed sensing with partially known support," in *ICASSP*, March 2010, pp. 3654–3657.
- [53] V. Stanković, L. Stanković, and S. Cheng, "Compressive image sampling with side information," in *IEEE International Conference on Image Processing (ICIP)*, Nov. 2009, pp. 3037–3040.
- [54] D. Cohen, K. V. Mishra, and Y. C. Eldar, "Spectrum sharing radar: Coexistence via xampling," *CoRR*, 2016.
- [55] C. Studer, P. Kuppinger, G. Pope, and H. Bolcskei, "Recovery of sparsely corrupted signals," *IEEE Trans. Information Theory*, vol. 58, no. 5, pp. 3115–3130, May 2012.
- [56] "Power systems test case archive." [Online]. Available: <http://www.ee.washington.edu/research/pstca/>
- [57] F. Aminifar, A. Khodaei, M. Fotuhi-Firuzabad, and M. Shahidehpour, "Contingency-constrained PMU placement in power networks," *IEEE Trans. Power Systems*, vol. 25, no. 1, pp. 516–523, Feb. 2010.
- [58] Q. Ding and S. Kay, "Inconsistency of the mdl: On the performance of model order selection criteria with increasing signal-to-noise ratio," *IEEE Trans. Signal Processing*, vol. 59, no. 5, pp. 1959–1969, May 2011.



Yonina C. Eldar (S98M02SM07-F'12) received the B.Sc. degree in Physics in 1995 and the B.Sc. degree in Electrical Engineering in 1996 both from Tel-Aviv University (TAU), Tel-Aviv, Israel, and the Ph.D. degree in Electrical Engineering and Computer Science in 2002 from the Massachusetts Institute of Technology (MIT), Cambridge. She is currently a Professor in the Department of Electrical Engineering at the Technion - Israel Institute of Technology, Haifa, Israel, where she holds the Edwards Chair in Engineering. She is also a Research Affiliate with the Research Laboratory of Electronics at MIT, an Adjunct Professor at Duke University, and was a Visiting Professor at Stanford University, Stanford, CA. Her research interests are in the broad areas of statistical signal processing, sampling theory and compressed sensing, optimization methods, and their applications to biology and optics.

Dr. Eldar has received many awards for excellence in research and teaching, including the IEEE Signal Processing Society Technical Achievement Award (2013), the IEEE/AESS Fred Nathanson Memorial Radar Award (2014), and the IEEE Kiyoo Tomiyasu Award (2016). She was a Horev Fellow of the Leaders in Science and Technology program at the Technion and an Alon Fellow. She received the Michael Bruno Memorial Award from the Rothschild Foundation, the Weizmann Prize for Exact Sciences, the Wolf Foundation Krill Prize for Excellence in Scientific Research, the Henry Taub Prize for Excellence in Research (twice), the Hershel Rich Innovation Award (three times), the Award for Women with Distinguished Contributions, the Andre and Bella Meyer Lectureship, the Career Development Chair at the Technion, the Muriel & David Jacknow Award for Excellence in Teaching, and the Technions Award for Excellence in Teaching (two times). She received several best paper awards and best demo awards together with her research students and colleagues including the SIAM outstanding Paper Prize, the UFFC Outstanding Paper Award, the Signal Processing Society Best Paper Award and the IET Circuits, Devices and Systems Premium Award, and was selected as one of the 50 most influential women in Israel.

She is a member of the Young Israel Academy of Science and Humanities and the Israel Committee for Higher Education, an IEEE Fellow, and a EURASIP Fellow. She is the Editor in Chief of Foundations and Trends in Signal Processing, a member of the IEEE Sensor Array and Multichannel Technical Committee and serves on several other IEEE committees. In the past, she was a Signal Processing Society Distinguished Lecturer, member of the IEEE Signal Processing Theory and Methods and Bio Imaging Signal Processing technical committees, and served as an associate editor for the IEEE Transactions On Signal Processing, the EURASIP Journal of Signal Processing, the SIAM Journal on Matrix Analysis and Applications, and the SIAM Journal on Imaging Sciences. She was Co-Chair and Technical Co-Chair of several international conferences and workshops.

She is author of the book "Sampling Theory: Beyond Bandlimited Systems" and co-author of the books "Compressed Sensing" and "Convex Optimization Methods in Signal Processing and Communications", all published by Cambridge University Press.



Tirza Routtenberg (S'07-M'13) received the B.Sc. degree (magna cum laude) in bio-medical engineering from the Technion Israel Institute of Technology, Haifa, Israel in 2005 and the M.Sc. (magna cum laude) and Ph.D. degrees in electrical engineering from the Ben-Gurion University of the Negev, Beer-Sheva, Israel, in 2007 and 2012, respectively. She was a postdoctoral fellow with the School of Electrical and Computer Engineering, Cornell University,

in 2012-2014. Since October 2014, she is a faculty member at the Department of Electrical and Computer Engineering, and Ben-Gurion University of the Negev, Beer-Sheva, Israel. Her research interests include signal processing in smart grid, statistical signal processing, and estimation and detection theory. She was a recipient of the Best Student Paper Award in International Conference on Acoustics, Speech and Signal Processing (ICASSP) 2011, in IEEE International Workshop on Computational Advances in Multi-Sensor Adaptive Processing (CAMSAP) 2013 (coauthor), and in ICASSP 2017 (coauthor). She was awarded the Negev scholarship in 2008, the Lev-Zion scholarship in 2010, and the Marc Rich foundation prize in 2011.